

# Use of Pulse- & Constant-current Plating for the Creation of Desirable Surface Microgeometry<sup>☆</sup>

By S.S. Kruglikov, P. Becker & O. Jankowski

The major factors responsible for favoring either non-uniform growth or smoothing a cathode surface microprofile are discussed. These include solution electrical resistance, diffusion of metal ions to the cathode, diffusion of other species to or from the cathode, and structural or chemical non-homogeneity of an electrodeposited surface. Electrodeposition of nickel on smooth and micro-rough surfaces was studied using low- and medium-frequency unipolar pulses under potenti- and galvano-static conditions.

Pulsing current is used in various electroplating processes to improve the properties of metal coatings. For example,

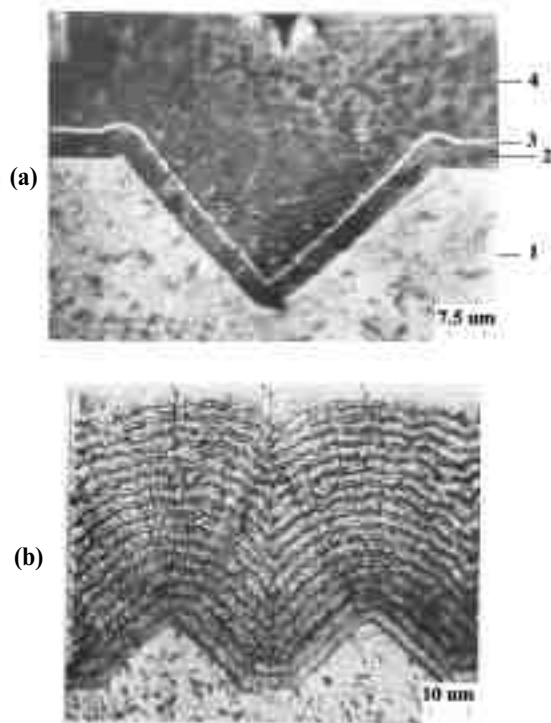


Fig. 1—Microsections of copper coatings deposited from solution #1 under conditions of uniform microdistribution (i.e., constant cathode current density of 5.0 A/dm<sup>2</sup> (46.5 A/ft<sup>2</sup>) with agitation). 1, electroformed nickel base; 2, copper layer; 3, intermediate nickel layer; 4, final protective copper layer [(Fig. 1(a)]. The specimen in Fig. 1(b) shows many layers that were made by interrupting the copper deposition in order to plate thin intermediate nickel layers using solution #4. These nickel layers were also deposited under conditions of uniform microdistribution. Their contrast with copper in the SEM makes this a useful technique for tracing the gradual evolution of microprofiles created during the course of metal (Cu) deposition.

<sup>☆</sup> Originally presented at SUR/FIN<sup>®</sup> 2000, Chicago, IL

in the manufacture of electrolytic copper foil, low-frequency (0.1 Hz) unipolar pulses have been used to create rough surface layers.<sup>1</sup> Conversely, under certain conditions pulsing improves coating brightness by planarizing cathode surfaces. Recently, the selection of pulse reverse parameters for plating electronic interconnects based on micro- and macro profiles has been discussed.<sup>2</sup> The effects of pulsing on the morphology of nickel deposits have also been reported recently.<sup>3,4</sup> The object of the present paper is to consider the major factors that control the evolution of a cathode surface microprofile during the course of electrodeposition including the role that current pulsing plays in this process.

## Background

### Voltage Drop & Throwing Power

The role that solution electrical resistance plays in any plating process can be expressed in terms of throwing power, or more correctly, in terms of Wagner's number.<sup>5</sup> This is defined as:

$$W = (|dE/di| \cdot \kappa) / L = K / L \quad (1)$$

where W is a dimensionless resistance parameter that is useful for evaluating electrochemical similarity<sup>6</sup> among different systems,  $|dE/di|$  is the cathode polarizability (where E is potential and i is current density),  $\kappa$  is solution conductivity, and L is the characteristic length, a linear value representing the shape and absolute dimensions of a particular electrolytic cell and all of its elements. The product  $(|dE/di| \cdot \kappa)$  defines the polarization parameter, K. For the majority of plating solutions, K values lie in a relatively narrow range, between 0.1 and 1.0 cm.<sup>7</sup> So Wagner's number in most systems will be dictated by the value of the characteristic length L, or more precisely, by the inverse of

## Nuts & Bolts: What This Paper Means To You

Pulse plating, around for years, offers the potential of producing plated metal properties and surfaces that can't normally be achieved by straight DC. The possibilities are endless, from copper foils, through electronic circuitry to decorative. Here, the authors consider how pulsing and constant current plating can achieve leveling and brightness. Putting the theory to practice here has the potential of operating with reduced levelers in certain applications. Could that Holy Grail of operating some baths without additives be far behind? By the way, Dr. Kruglikov will deliver the Blum Lecture at SUR/FIN '02.

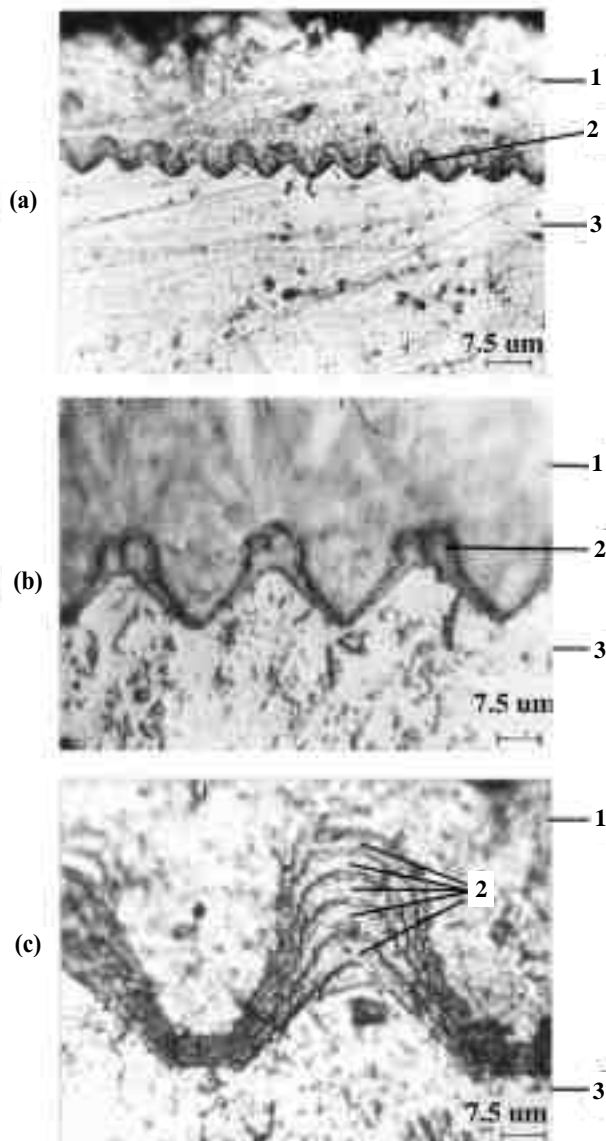


Fig. 2—Microsections of copper coatings deposited from solution #2 under conditions of high negative leveling (at a constant cathode potential of  $-0.3$  V (SHE), i.e., at a cathode overpotential of  $0.6$  V). 1, protective nickel coating; 2, copper layer; 3, electroformed nickel base metal. Deposition on a large scale profile [Fig. 2(c)] was interrupted and thin intermediate layers of nickel were deposited under conditions of uniform microdistribution.

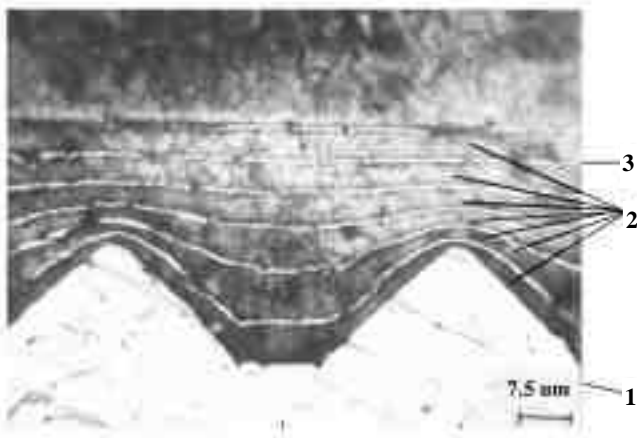


Fig. 3—Microsection of copper coating deposited from solution #3 under conditions of high positive leveling [ $3.0$  A/dm<sup>2</sup> ( $27.9$  A/ft<sup>2</sup>), agitation]. 1, electroformed nickel base; 2, copper layers; 3, intermediate thin nickel layers deposited under conditions of uniform microdistribution.

L. In the limit where the size of the cathode is small compared to (1) the distance between electrodes and (2) the distance between the cathode and the non-conductors (e.g., the surface of the solution, the walls and the bottom of the plating tank), L is solely determined by cathode geometry. The notion of L as a geometric parameter can be applied to any selected area of the cathode surface, (i.e., L changes in direct proportion with scale).

All plating processes, that is, any particular combination of cathode shapes and plating conditions (solution composition, temperature, average current density), fall within one of the following three limiting situations:

- (1)  $W \ll 1$  (i.e.,  $L \gg K$ )
- (2)  $W \sim 1$  (i.e.,  $L \sim K$  or  $0.1 < W < 10$ )
- (3)  $W \gg 1$  (i.e.,  $L \ll K$ )

For case (1), ohmic drop is the major factor that determines current distribution. Under these conditions, the values of local current densities are inversely proportional to the local solution resistances. This situation is referred to as “primary” current distribution. It is independent of the plating solution properties and is identical in all geometrically similar systems.

When W lies between 0.1 and 10, “throwing” action occurs [case (2)]. The resulting current distribution depends partly on ohmic drop, but is more uniform than it is in case (1). This situation is called “secondary” current distribution. Uniformity increases with higher values of W.

Conditions meeting the requirements for case (3) ( $W \gg 1$ ) typically occur with microprofiles ( $<0.01$  cm) where L values are very small.<sup>8</sup> These systems with high Wagner number values exhibit uniform current distribution. Ohmic factors cease to play a role at this scale. It should be noted that there are exceptions for certain types of microprofiles with unusually high L values. For example, L for pores or slots is determined by the ratio  $H^2/D$ , where H is the depth and D is the diameter or width. If  $H/D \gg 1$ , then L may correspond to macro- and not microregion behavior, even if the actual profile is at the microscale (where both H and D are below  $0.01$  cm). Plating on porous materials prepared from metal powders may be one practical example where this situation arises.

### Diffusion of Metal Ions

The rate at which metal ions diffuse to the cathode can have a significant effect on the distribution of metal deposition rates. These rates coincide with current distribution when current efficiency is close to 100 percent. The role played by the diffusion of metal ions becomes important in plating processes where the following condition arises:

$$i/i_{\text{lim}} > 0.1 \quad (2)$$

Here,  $i$  and  $i_{\text{lim}}$  are, respectively, the actual cathode current density and its limiting value or so-called diffusion current. At local sites where values of this ratio are higher than the average value for the whole cathode, metal deposition will be reduced. An example of this situation on the macroscale occurs in copper plating of high-aspect ratio through-holes on printed wiring boards (PWBs) where there is a lack of proper agitation. Typically, for this plating process, the sulfuric acid concentration is set at a high value (to increase solution conductivity,  $\kappa$ ) while that of copper sulfate is lowered (to increase cathode polarizability,  $(dE/di)$ ), in order to attain a high Wagner number. However, the combined effect of these altered concentrations also reduces  $i_{\text{lim}}$ , especially inside the through-holes. This can be overcome only if special arrangements are made for forced flow of plating solution into the through-hole regions. Metal ion diffusion can also play an important role in situ-

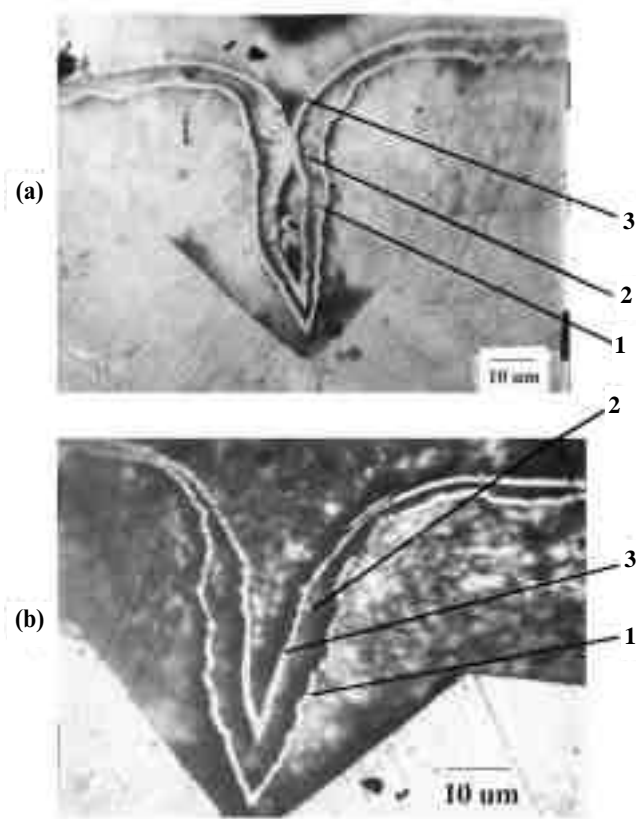


Fig. 4—Microsection of copper coating deposited from solution #3 with agitation at 20°C (68°F). 1, initial thin nickel layer deposited under conditions of uniform microdistribution; 2, copper layer as deposited from solution #3, (a) with current density = 8 A/dm<sup>2</sup> (74.3 A/ft<sup>2</sup>) and (b) with current density = 2 A/dm<sup>2</sup> (18.6 A/ft<sup>2</sup>); 3, top thin nickel layer deposited under conditions of uniform microdistribution.

ations where  $W < 1$ . If the local  $i/i_{lim}$  ratio is much higher than the average value, “burning” or spongy deposits will be formed at these sites. For cathode surfaces at the microscale level, a non-uniform distribution exists for both current and plated metal when  $i/i_{lim} > 0.3$ , even at high values of  $W$ . This non-uniformity arises from a local depletion of metal ions. Under these conditions, metal ions in the bulk solution diffuse more rapidly to microprotrusions than they do to microrecesses.

The dramatic effect that the  $i/i_{lim}$  ratio has on the growth of metal deposits is illustrated by comparing Figs. 1 and 2. For both of these examples,  $W \gg 1$ , meaning the ohmic drop did not affect current distribution. Figs. 1(a) and 1(b) contain microsections for two different samples plated under conditions where  $i/i_{lim} \ll 1$ . The “geometric” leveling exhibited in both cases is characteristic for microprofiles, because they evolve during the course of an electrodeposition process that is carried out under conditions of uniform microdistribution. Recesses or grooves present on the original surface gradually fill in and disappear, while initial protrusions expand both laterally and vertically, gradually increasing their radius of curvature. In contrast, Figs. 2(a-c) illustrate a strong negative leveling behavior that results from plating under conditions where  $i/i_{lim} \sim 0.8$ . The actual dimensions of the initial microprotrusions seen in these micrographs vary by almost a factor of 10. Yet, in all three cases, metal is preferentially deposited onto the high points of these microprofiles. It should be noted that this type of metal distribution occurs on geometrically similar microprofiles, even though the actual size scale for each may be quite different. In Fig. 2(c), evidence of continuous redistribution of the metal deposition rate can be seen as the micropeak develops and grows selectively during the course of electrodeposition. This inherently self-accelerating process is characteristic of negative leveling. Ultimately, deposition in the deep and narrow recessed areas stops altogether as they become completely shielded (by the growing peaks) from the supply of metal ions.

The relative difference between the local deposition rates at the

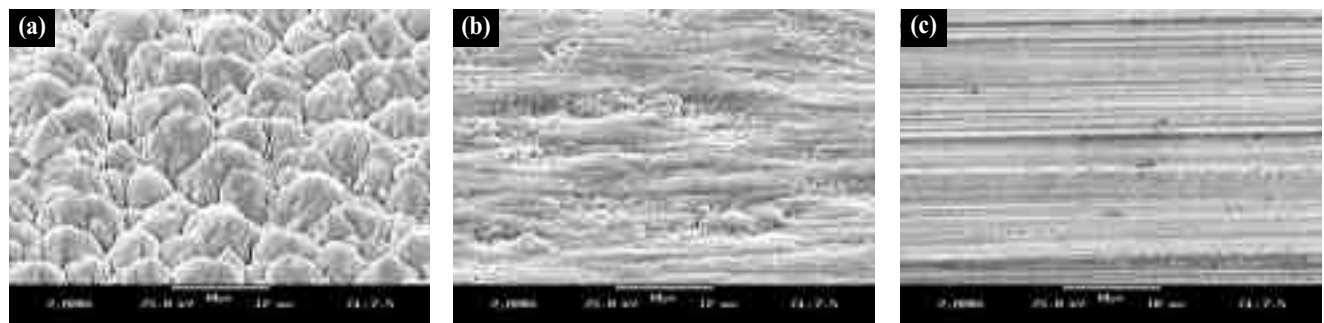


Fig. 5—Original cathode surfaces: (a) matte side of electrolytic copper foil; (b) shiny side of electrolytic copper foil; (c) rolled copper foil.

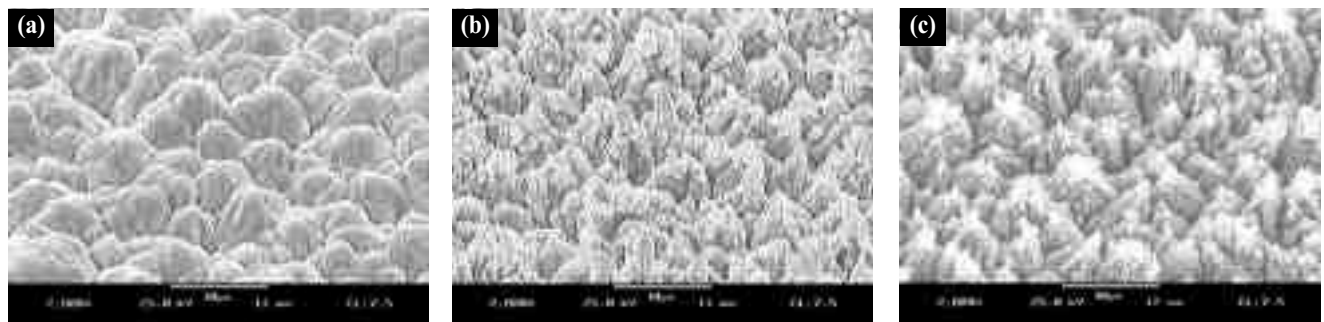


Fig. 6—Nickel deposited onto the matte side of electrolytic copper foil: (a) at constant potential (vs. SCE) of -1.0 V; current density was gradually decreasing from 0.5 to 0.3 A/dm<sup>2</sup> (4.6 to 2.8 A/ft<sup>2</sup>); Overall charge passed,  $Q = 600 \text{ coul/dm}^2$  (~5600 coul/ft<sup>2</sup>). (b) at constant potential (vs. SCE) of -1.3 V; current density was gradually decreasing from 2.1 to 0.9 A/dm<sup>2</sup> (19.5 to 8.4 A/ft<sup>2</sup>); Overall charge passed,  $Q = 600 \text{ coul/dm}^2$  (~5600 coul/ft<sup>2</sup>). (c) at approximately -1.8 V (vs. SCE); current density was gradually increasing from 9.0 to 10.2 A/dm<sup>2</sup> (83.6 to 94.8 A/ft<sup>2</sup>); Overall charge passed,  $Q = 300 \text{ coul/dm}^2$  (~2800 coul/ft<sup>2</sup>). Strong hydrogen evolution was observed.

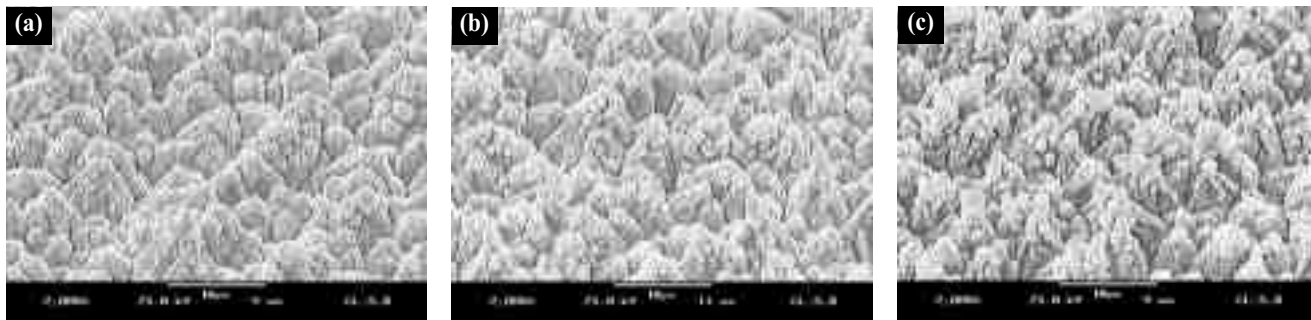


Fig. 7—Nickel deposited onto the matte side of ED Cu foil by alternating potentiostatic pulses: (a) -1.4V (5s) and -0.95V (20s);  $Q = 600 \text{ coul}/\text{dm}^2$  (~5600 coul/ft<sup>2</sup>). (b) -1.4V (10s) and -0.95V (20s);  $Q = 600 \text{ coul}/\text{dm}^2$  (~5600 coul/ft<sup>2</sup>). (c) -1.4V (20s) and -0.95V (20s);  $Q = 600 \text{ coul}/\text{dm}^2$  (~5600 coul/ft<sup>2</sup>).

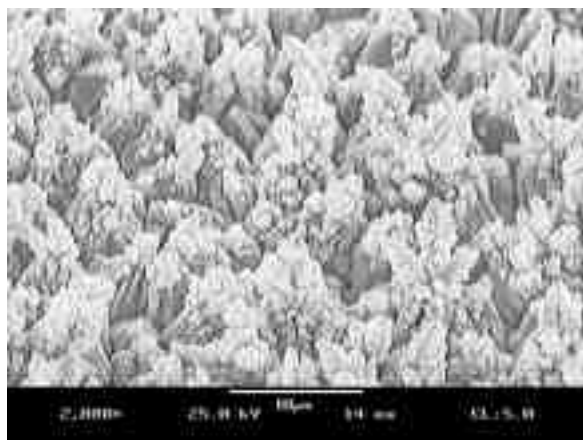


Fig. 8—Nickel deposited onto the matte side of ED Cu foil by alternating potentiostatic pulses: -1.4V (20s) and -0.95V (10s);  $Q = 600 \text{ coul}/\text{dm}^2$  (~5600 coul/ft<sup>2</sup>).

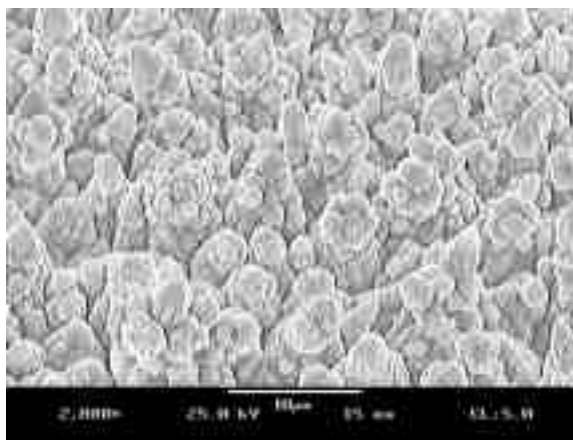


Fig. 9—Same as Fig. 6(c) with additional post-plated layer at -0.95V; additional  $Q = 300 \text{ coul}/\text{dm}^2$  (~2800 coul/ft<sup>2</sup>).

peaks ( $i_p$ ) and the recesses ( $i_r$ ) depends on the ratio of the height (H) and the width (a) of the surface irregularities. In the particular case of a sinusoidal microprofile with  $H/a \ll 1$  (“H” corresponding to the amplitude and “a” to the wavelength of the sinusoid), the microdistribution can be expressed by the following equation:<sup>9</sup>

$$(i_p - i_r) / i_{av} = -(4\pi H/a) \cdot P \quad (3)$$

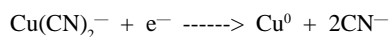
Here  $i_p$ ,  $i_r$  and  $i_{av}$  are the metal deposition rates (expressed in terms of current density) for a peak, a recess and the average value, respectively; and P is the leveling power of the plating solution. Evolution of the microprofile can be calculated by integrating equation (3):

$$\ln(H_l / H_0) = -(2\pi/a) \cdot P \cdot h \quad (4)$$

Here  $H_0$  and  $H_l$  correspond to initial and final amplitudes, respectively; and “h” is the average coating thickness. It follows from equations (3) and (4) that surface irregularities possessing smaller “a” values (narrow peaks) will grow faster than other surface features. This can be used to explain the mechanism of sponge or dendrite formation observed under conditions of limiting current density when the throwing power approaches -1. Fresh nuclei deposited as submicroprotrusions continuously appear and further develop by forming new dendritic branches via the accelerating effect of their smaller “a” values.

### Diffusion of Other Species

The metal deposition rate may also depend on the diffusion of such species as ligands, e.g.,  $\text{CN}^-$  anions which are released at the cathode during the reduction of copper cyanide solutions:



In this particular example, higher solution concentrations of  $\text{CN}^-$  will exist in the vicinity of the microrecesses due to the relatively slow rate that species diffuse away from these regions. This situation adversely affects leveling power and drives “P” to a more negative value. Because of this phenomenon, all plating solutions based on metal complexes inherently exhibit negative “P” values that must be altered by using special leveling additives. A recent example of the application of such additives has been described as it relates to copper plating of semiconductors.<sup>10</sup> Irrespective of the specific mechanism of their action, all leveling additives inhibit metal deposition and are consumed at the cathode. This inhibiting effect is stronger at sites where the rate of diffusion is higher, i.e., at protrusions or peaks. Therefore, leveling additives work by changing “P” in the direction of a more positive value. Figure 3 shows a microsection of a copper deposit obtained from solution #3 (see The table) that was prepared by adding a leveling agent to solution #1. Here, more metal is deposited in the valleys until they become filled in and the cathode surface becomes level.

In considering all of the above-discussed cases, it should be noted that any of them may occur simultaneously in different combinations. Fig. 4(a) illustrates this point. Here, positive throwing power (P) initially resulted in faster deposition of metal on the upper portion of the side walls of a groove. At same time, insufficient diffusion of metal ions and a higher ohmic resistance led to slower metal deposition at the bottom of the groove. These local differences in metal deposition rates continued to increase as the plating process progressed. Eventually, the opening at the top of the groove was narrowed and closed off so that metal deposition inside the cavity ceased altogether. This can be contrasted with the results shown in Fig. 4(b), where the same solution at a lower

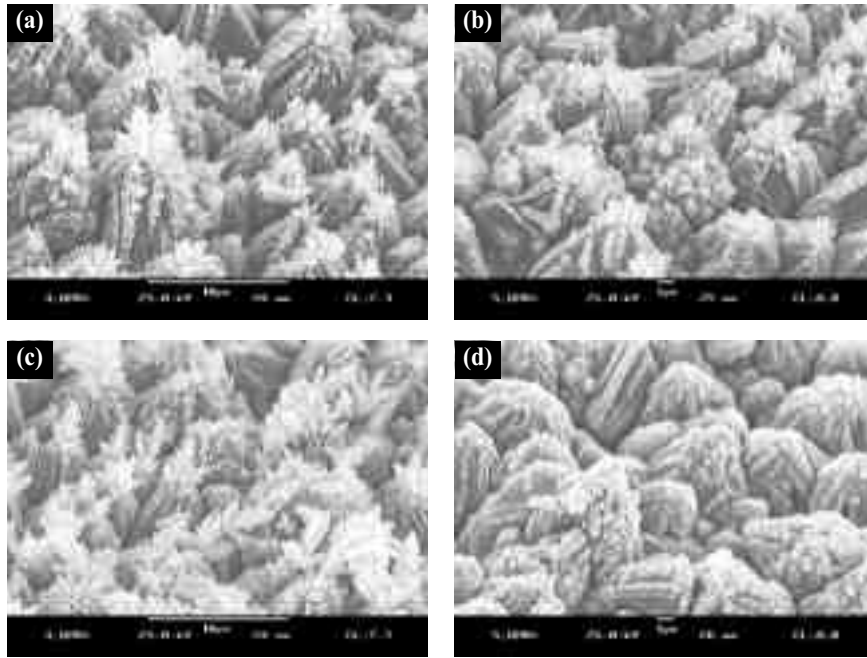


Fig. 10—Nickel deposited onto the matte side of ED Cu foil using: (a) galvanostatic pulses: 10 Hz; 25 A/dm<sup>2</sup> (232 A/ft<sup>2</sup>); 33% duty ( $t_{on}/t_{off} = 1:2$ );  $t = 34$  s ( $Q = 280$  coul/dm<sup>2</sup>; ~2600 coul/ft<sup>2</sup>). (b) galvanostatic pulses: 83 Hz; 25 A/dm<sup>2</sup> (232 A/ft<sup>2</sup>); 33% duty ( $t_{on}/t_{off} = 1:2$ );  $t = 34$  s ( $Q = 280$  coul/dm<sup>2</sup>; ~2600 coul/ft<sup>2</sup>). (c) DC at 25 A/dm<sup>2</sup> (232 A/ft<sup>2</sup>);  $t = 11$  s ( $Q = 280$  coul/dm<sup>2</sup>; 2600 coul/ft<sup>2</sup>). (d) galvanostatic pulses: 100 Hz; 25 A/dm<sup>2</sup> (232 A/ft<sup>2</sup>); 11% duty ( $t_{on}/t_{off} = 1:9$ );  $t = 100$  s ( $Q = 280$  coul/dm<sup>2</sup>; ~2600 coul/ft<sup>2</sup>).

average current density ( $i_{av} \ll i_{lim}$ ) completely filled in this groove without forming a cavity. Under these conditions, deposition at the bottom area of the groove was faster than at the upper portions.

### Electrocrystallization

Formation and growth of metal nuclei, *i.e.*, electrocrystallization, can be the source of so-called “crystalline roughness.”<sup>11</sup> All the above-discussed factors may contribute either positively or negatively to this process. Solution resistance and negative leveling accelerate growth of rough surfaces, while positive (or true) and geometric leveling has the opposite effect. Organic additives categorized as non-leveling brighteners function by suppressing the formation of crystalline roughness. Such additives can preserve the luster of the original substrate surface during electrodeposition, or even improve it through the effect of geometric leveling.

### Chemical Non-homogeneity of the Cathode Surface

In alloy plating processes, the chemical composition of deposits plated at the micropeaks may differ from that which is plated in the microrecessed regions. This non-homogeneity can result from diffusion limitations for one of the components in the plating solution.<sup>12</sup> Alloying components may act either as leveling agents (*e.g.*, cadmium ions in nickel plating solutions) or as anti-levelers (*e.g.*, copper ions in nickel plating solutions). In general, the mechanism here is similar to that for organic additives, a minor (diffusion-controlled) component either accelerates or inhibits the deposition of a major component of the alloy, resulting in negative or positive leveling, respectively.

### Role of Current Pulsing

Under non-steady-state conditions, all of the above-discussed factors may contribute to the microdistribution of metal deposition rates. The extent to which these factors contribute varies either continuously (as in medium- and high-frequency pulsing) or

periodically (as in low-frequency pulsing). High over-potential or high current density pulses tend to create diffusion limitations for metal ions and other species participating in cathodic deposition processes. Low over-potential or low current density pulses and off-time between pulses favor uniform microdistribution.

Reversed (or anodic) pulses may be used to create positive leveling known as electropolishing. This works by selectively removing (dissolving) the micropeaks on the substrate surface. However, the opposite effect may also occur if this process is applied in solutions containing leveling additives. Here, reversed pulsing counters the effect of these additives and can lead to an undesired surface finish. Pulse reverse plating has recently been reported to affect the current efficiency and throwing power during chromium plating.<sup>13</sup>

The proper choice of electrical parameters and time intervals in pulsed electrodeposition allows one to selectively change the morphology of the cathode surface, regardless of its original character. In the metal deposition experiments described below, we elected to use both electroformed and rolled copper foils as substrates because they provide

a wide range of surface microgeometries. These include a microrough ground surface found on the “shiny” side of electroformed foil, a high amplitude (several microns) rough crystalline surface present on the “matte” side of electroformed foil, and a very low amplitude microprofile found on the surface of rolled foil. These examples span the majority of substrate surfaces typically encountered in industrial electroplating. The complex interactions that occur between pulse frequency and hydrodynamically active additives have recently been reviewed.<sup>14</sup> To simplify the variables at this stage of our investigation, only solutions free of organic brightening or leveling additives were studied and only unipolar pulses of low and medium frequencies were used. In fact, two recent articles have suggested that the proper selection of pulse plating parameters could eliminate the need for additives.<sup>15,16</sup>

### Experimental Procedure

Electrodeposition experiments on foil substrates were carried out with one type of nickel bath (Solution #5)\*\* using either potentiostatic or galvanostatic equipment. Electrolytic copper foil (both matte and shiny sides) and rolled copper foil were used as cathode materials. Scanning electron micrographs of these cathode surfaces were taken at a 45° angle with respect to the sample plane and are shown in Fig. 5. All plating experiments were conducted at room temperature without agitation. Nickel foil was used as the anode. A saturated calomel electrode served as a reference and was placed about 1 mm from the cathode surface. Cathodic cur-

\*\*Solution #5 is a unique formulation for a high throw nickel bath. It was chosen for the following reasons: 1) a combination of low concentration of Ni ions (0.18 N) and nearly tenfold overall ionic concentration (1.6 N) eliminates ohmic factors in both the macro- and microdistribution over the surface microroughness; 2) a relatively low limiting current density is easily accessible with a potentiostat used as a source of pulsing current and 3) a high ammonium-to-nickel concentration ratio prevents the precipitation of nickel hydroxides generated at the cathode surface during hydrogen formation:  $2H_2O + 2e^- \rightarrow H_2 + 2OH^-$ .

rent efficiency was not determined, so the exact values of the average deposit thickness are unknown. It should be noted that at high values of cathode polarization the current efficiency was considerably lower than the 90 to 95 percent range that is typical for nickel plating at these pH values. The copper foil samples shown later in Fig. 10 were pre-plated with nickel at 0.25 A/dm<sup>2</sup> (2.3 A/ft<sup>2</sup>) immediately preceding the experiment ( $Q = 50 \text{ coul/dm}^2$ ; 464 coul/ft<sup>2</sup>).

## Results & Discussion

### Deposition Under Steady Potentiostatic Conditions

An initial series of plating experiments was carried out under potentiostatic conditions (Fig. 6) in order to determine the character of the micro-distribution of nickel at different cathode potentials. These conditions corresponded to current density regimes that were (1) much less than, (2) comparable to and (3) much greater than the limiting current. This last condition resulted in a much lower plating efficiency, so the amount of electric charge passed during electrolysis did not accurately reflect the quantity of plated nickel. Nevertheless, dramatic changes in the surface morphology were observed in this particular sample [Fig. 6(c)]. It was covered by a very fine bushy deposit. This contrasted with low polarization conditions [Fig. 6(a)] where the original microgeometry underwent only minor changes consistent with geometric leveling, *i.e.* the filling of narrow recesses along with uniform nickel deposition on flat surfaces. The intermediate condition [Fig. 6(b)] represented strong anti-leveling conditions where there was a transition from dense to spongy deposits. Branched dendrites have grown on the tops of the original copper peaks (where the diffusion flow of nickel ions is most favorable), while very little nickel appears to have coated the base of the peaks that make up a major portion of the cathode surface.

Using these initial results as a guideline, we carried out a subsequent series of plating experiments using potentiostatic pulses that alternated between the extremes of  $-0.95 \text{ V}$  and  $-1.40 \text{ V}$ .

### Deposition Using Potentiostatically Controlled Alternating High- & Low-polarization Pulses (<0.1 Hz)

A series of plating experiments was performed using rectangular unipolar current pulses at frequencies ranging from 0.040 - 0.025 Hz (Fig. 7). Low polarization pulses of long duration were used to ensure sufficient time for the concentration of nickel ions near the cathode surface (both peaks and valleys) to approach to bulk values. As a consequence, the subsequent high-polarization pulses resulted in the formation of three-dimensional nuclei over much of the cathode surface. The principal difference between Figs. 7(a) and 7(c) was the ratio of nickel deposited under conditions of high anti-leveling to that deposited with uniform microdistribution. When this ratio was small [Fig. 7(a)], uniform microdistribution dominated the formation of the deposit morphology. It should be noted that even at the highest ratio [Fig. 7(c)], relatively few individual tree-like deposits had grown on the tops of the copper peaks. This differs from the results obtained in the previous potentiostatic experiment [Fig. 6(b)], even though it was conducted at a slightly lower polarization ( $-1.3 \text{ V}$  vs.  $-1.4 \text{ V}$ ).

## Plating Bath Compositions

Component	Concentration (mole/L)				
	Soln. #1	Soln. #2	Soln. #3	Soln. #4	Soln. #5
CuSO <sub>4</sub> ·5H <sub>2</sub> O	1.0	0.2	1.0		
H <sub>2</sub> SO <sub>4</sub>	0.5	1.7	.05		
NiSO <sub>4</sub> ·6H <sub>2</sub> O				0.89	0.09
NiCl <sub>2</sub> ·6H <sub>2</sub> O				0.17	
NaCl					0.17
H <sub>3</sub> BO <sub>3</sub>				0.49	0.20
Na <sub>2</sub> SO <sub>4</sub>					0.17
(NH <sub>4</sub> ) <sub>2</sub> SO <sub>4</sub>					0.11
Proprietary leveler + brightener (mL/L)			6		
Temperature, °C	18-20	18-20	18-20		20 - 25

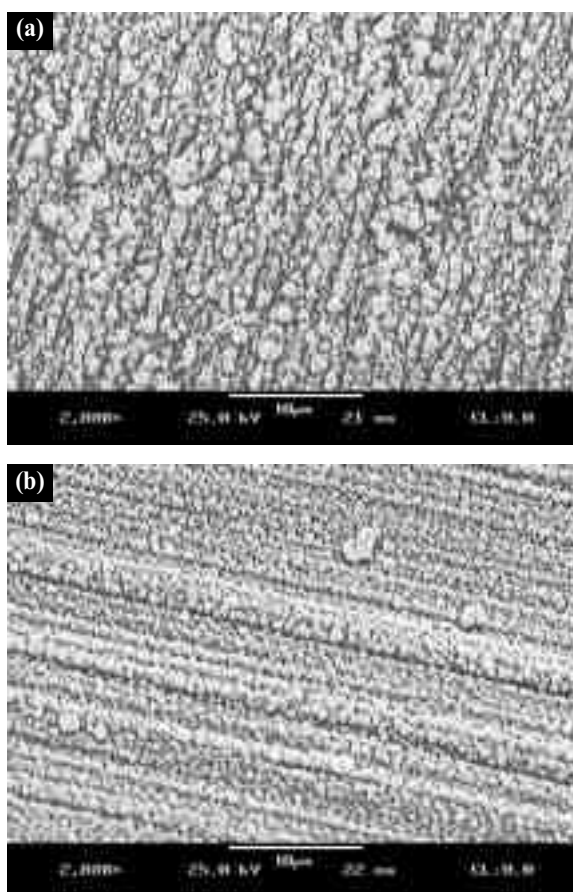


Figure 11 - (a) Nickel deposited onto the shiny side of ED Cu foil by galvanostatic pulses: 83 Hz; 25 A/dm<sup>2</sup> (232 A/ft<sup>2</sup>); 33% duty ( $t_{on}/t_{off} = 1:2$ );  $t = 34s$  ( $Q = 280 \text{ coul/dm}^2$ ; ~2600 coul/ft<sup>2</sup>), (b) Nickel deposited onto rolled Cu foil by galvanostatic pulses: 83 Hz; 25 A/dm<sup>2</sup> (232 A/ft<sup>2</sup>); 33% duty ( $t_{on}/t_{off} = 1:2$ );  $t = 34s$  ( $Q = 280 \text{ coul/dm}^2$ ; ~2600 coul/ft<sup>2</sup>).

The surface morphology obtained by the pulse plating process can easily be altered by the addition of a subsequent direct current-plating step. Figures 8 and 9 illustrate this point. Initially, nickel was pulse-plated under conditions which favored strong dendritic growth, *i.e.*, using a high ratio of  $t_H/t_L = 20s/10s = 2.0$  (Fig. 8). In a second step, additional metal was plated from the same solution at a constant low-polarization potential (Fig. 9). The amount of nickel

deposited under this condition of uniform microdistribution corresponded to an average thickness of about 1  $\mu\text{m}$ .

### Medium Frequency Galvanostatic Pulsed Plating (10 – 100 Hz)

Electrode potentials do not decay instantaneously during the off-time of a pulsed plating cycle<sup>17</sup>. Some charge remains stored in the double-layer capacitor at the cathode/solution interface. This capacitor discharges by reducing metal ions at the interface. As a result, metal deposition takes place during the off-time as the cathode potential gradually decays below the limiting value. At higher frequencies, metal deposition under these circumstances becomes more important, because a significant fraction of the deposit is plated during the “off” period. In our experiments, the decay portion of the pulse cycles effectively functioned as a substitute for the long duration, low-polarization pulses used in the preceding potentiostatic experiments. By varying pulse current amplitudes and the ratio of  $t_{\text{on}}/t_{\text{off}}$ , it is possible to adjust the average current density as defined in equation (5).

$$i_{\text{AV}} = [i_{\text{pulse}}] \cdot [t_{\text{on}} / (t_{\text{on}} + t_{\text{off}})] \quad (5)$$

Likewise, both the average concentration gradient in the diffusion layer and the total amount of metal deposited under non-diffusion-controlled conditions are influenced by the ratio  $i_{\text{AV}}/i_{\text{lim}}$ . For example, if the objective is to produce rough deposits evenly over a non-flat surface (like matte Cu foil), then major efforts should be directed toward the proper choice of plating parameters, which ensures maintenance of the inequality shown in equation (6).

$$i_{\text{AV}} < 20\text{-}33\% \text{ of } i_{\text{lim}}. \quad (6)$$

Our initial unipolar pulse plating experiments using a 33 percent duty cycle [Figs. 10 (a) and (b)] produced nodular and dendritic deposits that were similar in size and shape to those obtained in the corresponding DC experiment [Fig. 10(c)]. The main difference was that the pulsed samples contained less nickel deposit, a result of lower current efficiency under these conditions. However, when  $i_{\text{AV}}$  was decreased by a factor of three (by lowering the duty cycle to 11%), a spectacular change in deposit morphology took place. The substrate was populated only with nodules. Not a single dendrite had formed on the tops of the copper peaks [Fig. 10(d)].

It should be noted that controlling dendritic growth on the matte side of electrolytic copper foil is more difficult than doing so on smoother substrates, such as rolled foil or the shiny side of electrolytic foil. Figure 11 illustrates this point by showing that nodular deposits were obtained on these substrates, even at 33 percent duty cycle. The starting surfaces for these samples lacked the large asperities found on matte copper foil that act as initiation points for preferential and auto-accelerating growth of tall, branched dendrites.

### Conclusions

1. We have observed that different types of galvanostatic and potentiostatic current pulses can be used to vary the electrodeposit microdistribution ranging from uniform to strongly anti-leveling.
2. Discharge of metal ions can be directed to occur at specific sites on the cathode surface by using pulsed currents and proper bath formulations (e.g., by introducing leveling additives).
3. Medium-frequency pulses can be used to reduce the amplitude of rough electrodeposits by keeping the average deposition current below the limiting value.

### References

1. S.S. Kruglikov, T.A. Vagramyan, *Zhurnal Vses. Khim. Obsh. (J. Chem. Soc. USSR)*, **33**, 164 (February 1988).
2. E.J. Taylor, J.J. Sun, M.I. Inman, *Plating & Surface Finishing*, **87**, 68 (December 2000).
3. S.S. Kruglikov, R.A. Novozhilova, S.M. Kornilova, *Proc. AESF SUR/FIN '98*, 173 (1998).
4. S.S. Kruglikov, P. Becker, O. Jankowski, *Proc. AESF SUR/FIN '00*, 673 (2000).
5. C. Wagner, *J. Electrochem. Soc.*, **98**, 116 (1951).
6. S.S. Kruglikov, E.S. Kruglikova, *Proc. AESF SUR/FIN '96*, 819 (1996).
7. V.N. Golubev, N.Ya. Kovarski, *Microgeometry of Electrodeposited Surfaces* (in Russian), Siberian Div. of the USSR Academy of Sci., Novosibirsk, 1970.
8. O. Kardos, D.G. Foulke, *Advances in Electrochemistry and Electrochemical Engineering*, **2**, P. Delahay and C. W. Tobias, eds., Wiley-Interscience, New York, NY, 1962; p. 145.
9. S.S. Kruglikov, T.A. Smirnova, *Proc. INTERFINISH Conf.*, Basel, 1972, 105 (1973).
10. R.D. Mikkola, Q.T. Jiang, B. Carpenter, *Plating & Surface Finishing*, **87**, 81 (March 2000).
11. S.S. Kruglikov, N.Ya. Kovarski, *Itogi Nauki. Khimiya. Elektrokimiya (Achievements in Science. Chemistry. Electrochemistry)*, **10**, 106 Moscow, VINITI (1975).
12. S.S. Kruglikov, V.I. Kharlamov, T.A. Vagramyan, *Trans. IMF*, **74**, Part 6, 189 (November 1996).
13. D.L. Rehrig, N.V. Mandich, *Plating & Surface Finishing*, **86**, 89 (December 1999).
14. M.S. Aroyo, *Plating & Surface Finishing*, **82**, 53 (November 1995).
15. E.J. Taylor, *Plating & Surface Finishing*, **87**, 118 (May 2000).
16. E.J. Taylor, *Plating & Surface Finishing*, **87**, 56 (July 2000).
17. J. Puipe & F. Leaman, eds., *Theory and Practice of Pulse Plating*, AESF, Orlando, FL, 1986; p. 41.

### About the Authors



S.S. Kruglikov



P. Becker



O. Jankowski

*Dr. Sergei S. Kruglikov\* is president of S.S. Kruglikov Consultants, Kv 107, Bolshaya Spasskaya, Moscow, Russia 129090. He has participated in numerous projects with educational and industrial institutions both in Russia and abroad. He graduated from the Mendeleev Institute of Chemical Technology in Moscow and obtained his doctorate degree in electrochemical engineering from the same institution.*

*Dr. Paul Becker is a research manager working for Tyco Electronics. He obtained a BA from Columbia University and a PhD in chemistry from UC Berkeley.*

*Orion Jankowski was a summer intern for Tyco Electronics while he contributed to work presented in this paper. He holds a BS from UC Berkeley and is currently pursuing a PhD in chemistry at Stanford University.*